Novel 6-DoF dexterous parallel manipulator with CRS kinematic chains

†M.A. Hosseini[1]

[1]Department of Mechanical Engineering, University of Mazandaran, Babolsar, Iran.

*Presenting author: ma.hosseini@umz.ac.ir
†Corresponding author: ma.hosseini@umz.ac.ir

Abstract

In this research work, a novel parallel manipulator with 6 degrees of freedom (DoF) and high positioning and orienting rate is introduced. Kinematics and Jacobian analysis are investigated. Workspace of mechanism considering different rotation capabilities are computed and illustrated in Cartesian coordinates. Defining *global maximum* and *minimum singular values* of homogenized jacobian matrix through the workspace has been utilized in order to synthesis positioning and orienting rates capability of mechanism. Thus, improving high rates of displacement is achieved by elimination of moving elements and changing kinematic chains compared with general stewart-gough mechanism, which makes it suitable in pick and place or motion stabilizer devices and high speed machining applications with lower payload**.**

Keywords: Kinematics, Workspace, 6-CRS, Parallel robot.

Introduction

Potential superior properties of parallel manipulators such as low inertia, high stiffness, high precision and high load carrying capacity [1]-[2] of parallel manipulators lead to extensive attention over the last three decades of them. Performance indices such as manipulability, condition number, conditioning and dexterity are useful for comparison studies of different robot structures. Manipulability at first was introduced by Yoshikawa [3] as the square root of the determinant of the product of the manipulator Jacobian by its transpose.

The Jacobian matrix maps a unit ball in the joint space into a rotated or reflected ellipsoid in the Cartesian space. The geometric interpretation of the mapping is proportional to the volume of the ellipsoid or the manipulability [3]. Moreover, the volume is equal to the products of the singular values of the Jacobian [3]. Salisbury and Craig [4] introduced the ratio between the maximum and minimum singular values as the condition number. The inverse of the Euclidean condition number is defined as conditioning index which varies from 0 to 1. if the entries of the Jacobian have different units for the manipulators with both positioning and orientation tasks, which is the case here, one faces a problem of ordering singular values of different units from largest to smallest. Ranjbaran and Angeles [5] introduced carachteristic length to resolve this issue. Gosselin [6] introduced a method for formulating dimensionally homogeneous Jacobian matrix for a planar mechanism with one rotational and two translational degreeof-freedom (dof). Kim and Ryu [7] furthered this work by using the velocities of three points on the endeffector platform to develop a dimensionally homogeneous Jacobian matrix. Pond and Corretero [8] furthered this method again by using three independent coordinates of three points on an end-effector platform. Moreover, Angeles [9] introduced engineering characteristic length for a rigid body transformation matrix to make it homogeneous. Finally, Hosseini et. al. [10]-[11], introduced a weighting factor method to make it homogeneous.

Here a novel mechanism with high positioning and orienting rate is introduced. Its kinematic is studied and its Jacobian matrices are derived from these equations. Because of complexity of DoF, Jacobian matrix is homogenized by using weighted factor method [10].

Moreover, kinematic indices for a trajectory have been investigated and compared with the similar size of stewart-gough mechanism, as a case study. Although decreasing the moving elements leads to better dynamic performances, this investigation could demonstrate kinematic indices improvement due to structural transformation at all.

I. 6-CRS Parallel Manipulator

As depicted in Fig. 1, 6-CRS parallel manipulator consists of two platforms connecting to each other by six identical active C-R-S (Cylindrical-Revolute-Spherical) legs. The active legs consist of a fixed length link connected to the mobile platform by a passive spherical joint. On the other extremity of the leg there is an actuated prismatic joint followed by a passive revolute joint.

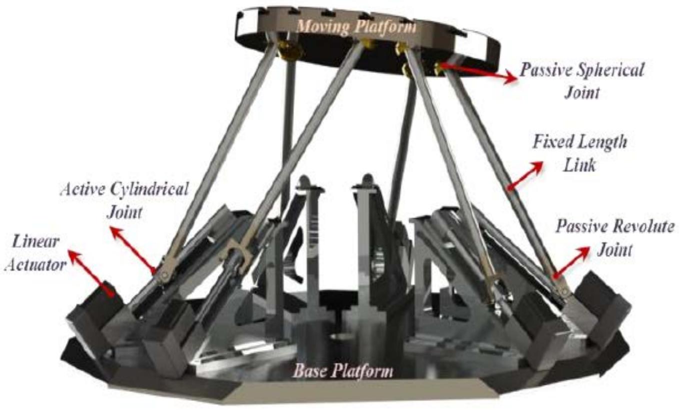

Figure 1. CAD model of 6-CRS parallel manipulator

II. Kinematic Analysis

Geometrical model of the mechanism is illustrated in Fig. 2. Two moving and global frames ({P (uvw)} and {O (xyz)}) are attached to the moving and base platforms, respectively.

The kinematic close loop equation can be written as follow for each leg:

$$\mathbf{x} + a\mathbf{R}\mathbf{n}_{ai} = b\mathbf{n}_{bi} + q_i \mathbf{n}_{qi} + l\,\mathbf{n}_{li} \quad . \tag{1}$$

where $\mathbf{x}$ is the vectors from O to P, i.e. the end effector position vector. Moreover, $\mathbf{R}$ is rotation matrix carrying frame {P} into an orientation coincident with that of frame {O}; $\mathbf{n}_{ai}$ is the i^{th} spherical joint position unit vector in the moving frame. Similarly, $\mathbf{n}_{bi}$, $\mathbf{n}_{qi}$ and $\mathbf{n}_{li}$ are the unit vectors from O to B_i, B_i to Q_i and Q_i to A_i, respectively; while a and b are the radius of the moving and base platform that joints are posed on. Furthermore, the moving part of the limbs length is l.

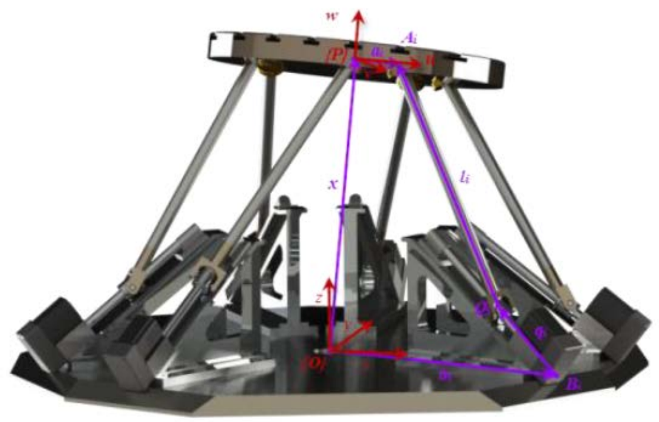

Figure 2. Geometrical Model of 6-CRS

A. Inverse Kinematic

In the Inverse kinematic problem the pose of the end-effector (EE) is given and the joint variables that produce this pose are to be found. Considering the i^{th} leg as depicted in Fig. 3; it is obvious that Q_i is on the surface of a sphere with the centre A_i and radius of l. Then the intersection of this sphere with the slant base concludes the inverse kinematic problem roots.

The position vector of A_i can be defined by the following equation.

$$\mathbf{a}_i = \mathbf{x} + a\mathbf{R}\mathbf{n}_{ai} \ . \tag{2}$$

Considering spherical and universal joints position vector as $\mathbf{a}_i=[x_{ai}\ y_{ai}\ z_{ai}]^T$ and $\mathbf{b}_i=[x_{bi}\ y_{bi}\ 0]^T$ the parametric equation of GB_i can be written as follow, in which the intersection of all slant bases is illustrated by G.

$$x = -x_{bi}t_i + x_{bi} ; y = -y_{bi}t_i + y_{bi} ; z = ht_i \tag{3}$$

where h is the height of G point.

Substituting the above equations in the parametric equation of sphere as the following:

$$(x - x_{ai})^2 + (y - y_{ai})^2 + (z - z_{ai})^2 - l^2 = 0 \tag{4}$$

Leads to the following equation

$$m_i t_i^2 - 2n_i t_i + p_i = 0 \tag{5}$$

In which coefficients are given as:

$$m_i = (x_{bi}^2 + y_{bi}^2 + h^2) \tag{6}$$

$$n_i = (x_{bi}^2 + y_{bi}^2 - x_{bi}x_{ai} - y_{bi}y_{ai} + hz_{ai}) \tag{7}$$

$$p_i = (x_{bi}{}^2 + x_{bi}{}^2 - 2x_{bi}x_{ai} + y_{bi}{}^2 + y_{ai}{}^2 - 2y_{bi}y_{ai} + z_{ai}{}^2 - l^2) \tag{8}$$

Solving Eq. (5) for t_i and substituting the values of Eq. (3) led to the inverse kinematic problem solution. This approach could help to avoiding impossible roots such as R_{i2} in Fig 3. Thus, only the roots are acceptable in which associated t_i lie in desired interval satisfied by the linear actuator stroke.

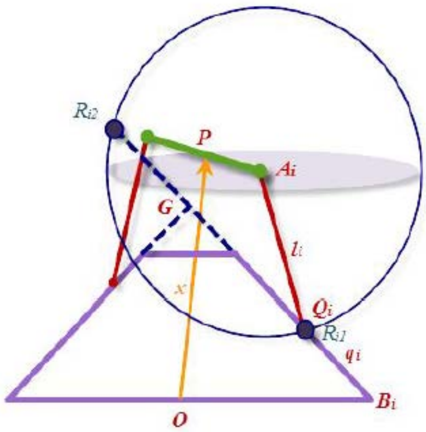

Figure 3. Schematic configuration of 6-CRS kinematic

The following cases may occur:

Case 1) The slant guide way does not intersect the associated sphere. Thus there is no solution for IKP (Inverse Kinematic Problem), i.e., the assumed position would be out of reach by the EE(End Efector).

Case 2) The slant guide way intersects with the associated sphere at one point. Therefore, IKP leads to only one solution for the corresponding leg.

Case 3) The slant guide way intersects with the associated sphere at two points. Therefore, IKP leads to two solutions for the corresponding leg, as depicted in Fig 3, by R_{i1} and R_{i2}.

Therefore, the IKP might leads to 2^6 solutions (with considering dual roots) or no solution at all.

III. Jacobian Matrix and Velocity Analysis

The first time derivative of Eq. (1) leads to:

$$\dot{\mathbf{x}} + \boldsymbol{\omega}_p \times a\mathbf{R}\mathbf{n}_{ai} = \dot{q}_i \mathbf{n}_{qi} + \boldsymbol{\omega}_l \times \mathrm{l}\,\mathbf{n}_{li} \tag{9}$$

In which $\boldsymbol{\omega}_l$ and $\boldsymbol{\omega}_p$ are the angular velocities of the fixed length link and the moving platform, respectively. Inner product of the both sides of Eq.9 by $\mathbf{n}_{li}$, upon simplifications leads to:

$$\dot{\mathbf{x}}\mathbf{n}_{li}{}^T + \boldsymbol{\omega}_p \times a\mathbf{R}\mathbf{n}_{ai}\mathbf{n}_{li}{}^T = \dot{q}\mathbf{n}_{qi}\mathbf{n}_{li}{}^T \tag{10}$$

Equation (10) can be rewritten as bellow

$$\mathbf{n}_{li}^{T}\dot{\mathbf{x}} + a(\mathbf{n}_{li} \times \mathbf{R}\mathbf{n}_{ai})\boldsymbol{\omega}_{p} = \dot{q}\mathbf{n}_{li}^{T}\mathbf{n}_{qi} \tag{11}$$

Writing the foregoing equation for the three legs yields to:

$$\mathbf{A}\dot{\mathbf{x}} = \mathbf{B}\dot{\mathbf{q}} \tag{12}$$

In which $\dot{\mathbf{x}}$ and $\dot{\mathbf{q}}$ are EE twist array and joint space velocity vector, respectively. Moreover, **A** and **B** are two Jacobian matrices which are given as:

$$\mathbf{A} = \begin{bmatrix} \mathbf{n}_{li} & \mathbf{n}_{li} \times a\mathbf{R}\mathbf{n}_{ai} \end{bmatrix}_{6\times 6} \tag{13}$$

$$\mathbf{B} = \begin{bmatrix} \mathbf{n}_{l1}^{T}\mathbf{n}_{q1} & 0 & 0 \\ \vdots & \ddots & \vdots \\ 0 & 0 & \mathbf{n}_{l6}^{T}\mathbf{n}_{q6} \end{bmatrix} \tag{14}$$

The Jacobian matrix can be determined by Eq. 15.

$$\mathbf{J} = \mathbf{B}^{-1}\mathbf{A} \tag{15}$$

IV. Singularity Analysis

Generally, singularity occurs whenever the manipulator loses some DoF or gains some uncontrollable DoF. In parallel manipulators singularities occur whenever **A**, **B** or both become singular. Thus, for the manipulator at hand a distinction can be made among three types of singularities, which have different kinematic interpretations.

For the 6-CRS parallel manipulator, singularity occurs in four cases, namely;

Case 1) First type of singularity or Inverse Singularity; in this case **B** is invertible and **A** is singular, i.e. when

$$\det(\mathbf{B}) = 0 \,\&\, \det(\mathbf{A}) \neq 0 \tag{16}$$

The physical condition happens when one of the fixed length link is perpendicular to the direction of the associated linear guide way.

Case 2) Second type of singularity or Direct Singularity; arises when **B** is singular and **A** is invertible, i.e. when

$$\det(\mathbf{B}) \neq 0 \,\&\, \det(\mathbf{A}) = 0 \tag{17}$$

This case occurs when the z coordinates of the fixed-length links vector is equal to zero. In this condition all three legs lie in the plane of the moving platform which is parallel to the base one, as well. Hence, by increasing or decreasing the actuator length, there are two options for A_i to locate, as depicted in Fig. 4, by 1 and 2.

Case 3) Third type of singularity; this type of singularity arises even if both **B** and **A** are simultaneously singular. Under a singularity of this type the manipulator can undergo finite motions even if the actuators are locked. As well, a finite motion of actuators produces no motion for EE in some directions.

Case 4) Constraint singularity; this case will occur when the moving platform rotates 90 degrees around x or y axis. In this case the platform will lose one rotational dof. Zalatanov et. al. [12] illustrated some constraint singularities, as well.

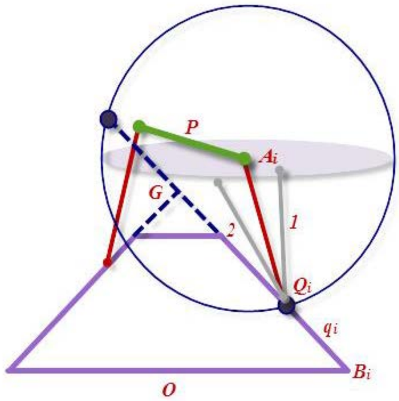

Figure 4. Schematic for direct singularity

V. Workspace and Optimization

Applying the inverse kinematic equations and a search algorithm in different height leads to the bound of reachable workspace [13]. This operation will be continuing as the geometric constraints are satisfied, subject to Table 1.

Table 1. Geometrical constraint for mechanism

Actuator (mm)	*l (mm)*	*λ (deg)*	*b (mm)*	*a (mm)*
0-600	*100-300*	*10-80*	*300-500*	*100-300*

As a case study, the Cartesian workspace of the structure according to Table 2, with the foregoing constraints is depicted in Fig. 5 in which the workspaces are depicted considering different rotation capabilities around three axes. Moreover, sub workspaces include bounded local conditioning indices into a minimum allowable of 0.0003 are depicted in Fig. 6 which singularity avoidance is performed.

Table 2. The case study design parameters

l (mm)	*λ (deg)*	*b (mm)*	*a (mm)*
300	30	300	100

Considering 100 (mm) weight factor for homogenized jacobian matrix, for the workspace with 20 degree rotation capability, the performance indices such as global conditioning index (GCI), average minimum and maximum singular values are depicted in Table 3.

Table 3. The case study performance indices

$V(mm^3)$	GCI	$\bar{\sigma}_{\max}$	$\bar{\sigma}_{\min}$
6.51e+6	0.9895	1.5016e+4	2.5899

Global conditioning index (GCI) [6], are defined as following equations.

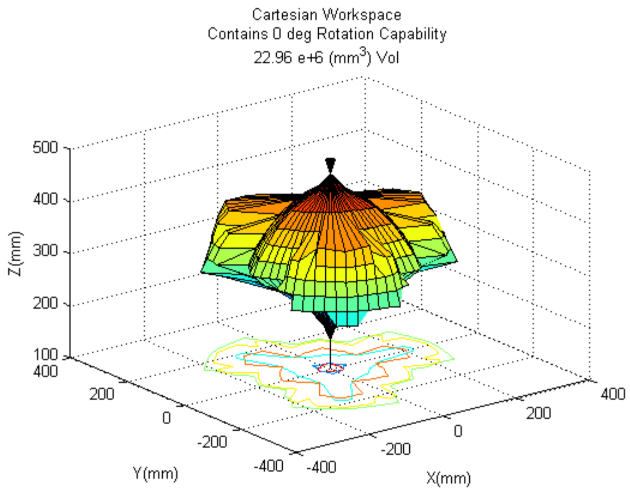

a. *0 deg Rotation Capability Cartesian Workspace*

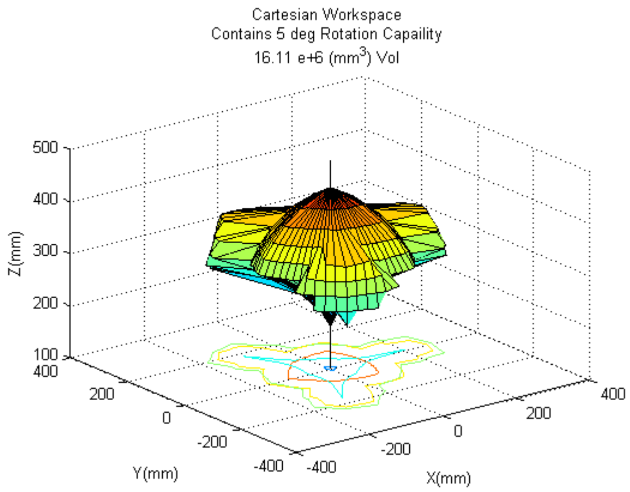

b. *5 deg Rotation Capability Cartesian Workspace*

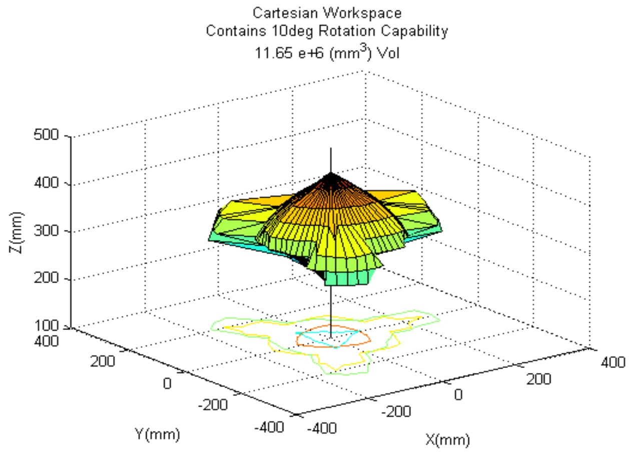

b. *10 deg Rotation Capability Cartesian Workspace*

Figure 5. The case study workspaces with different rotation capabilities

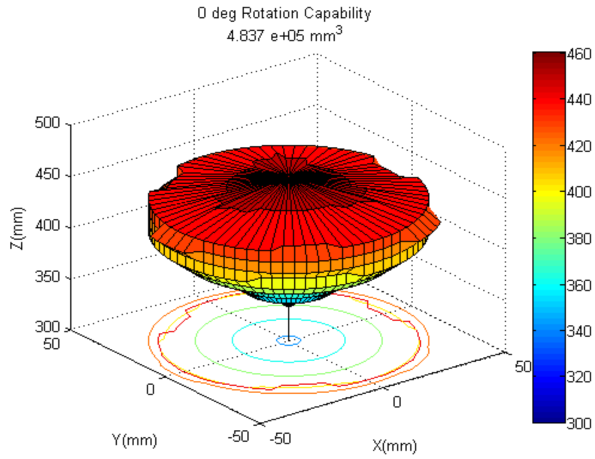

d. *Subworkspace with 0 deg Rotatioon Capability with minimum 0.0003 LCI*

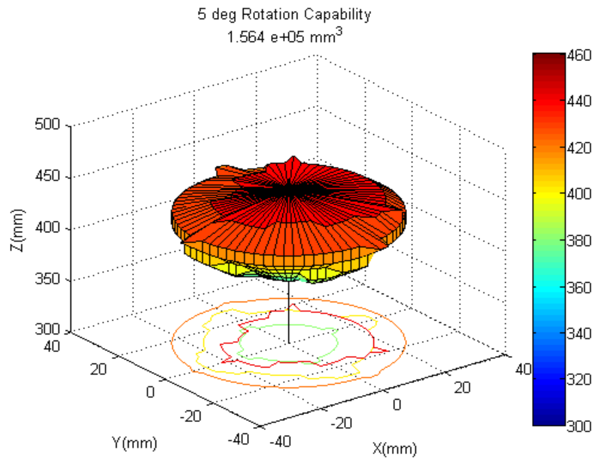

e. *Subworkspace with 5 deg Rotatioon Capability with minimum 0.0003 LCI*

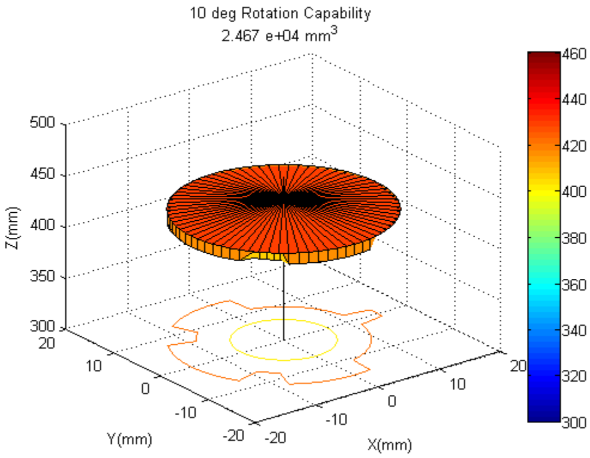

f. *Subworkspace with 10 deg Rotatioon Capability with minimum 0.0003 LCI*

Figure 6. Sub workspaces with different rotation capabilities

$$GCI = \frac{\int \kappa dv}{\int dv} \tag{18}$$

In which local conditioning index (κ) for the workspace element is determined by the respective of minimum and maximum singular values of homogenized jacobian matrix using weighted factor method.

$$\kappa = \frac{\sigma_{\min}}{\sigma_{\max}} \tag{19}$$

Respectively, the average maximum singular value and average minimum singular value indices as the performances indices for positioning and orienting rates are defined as follow.

$$\bar{\sigma}_{\max} = \frac{\int \sigma_{\max} dv}{\int dv} \tag{20}$$

And

$$\bar{\sigma}_{\min} = \frac{\int \sigma_{\min} dv}{\int dv} \tag{21}$$

Lower value of $\bar{\sigma}_{\max}$ led to higher end-effector positioning and orienting resolution and higher value of $\bar{\sigma}_{\min}$ led to higher positioning and orienting rates [6].

Conclusions

In this research work a novel parallel manipulator with 6-CRS kinematic chains is introduced. The mechanism has 6 degrees of freedom. Inverse kinematic equations with a geometrical approach have been solved and used to workspace evaluation. Proposed parametric solution method leads to avoidance of actuators to locate into other inverse kinematic solutions sets. Jacobian matrix is derived by taking the first time derivation respect to time. Jacobian entries inhomogeneity has resolved by weighted factor approach equal with moving platform radius. Considering minimum desired rotation angles workspaces estimated in Cartesian workspaces. Bounding minimum local conditioning indices to the minimum allowable value led to sub workspaces with different rotation capabilities. Finally for the case study structure, some global indices are calculated in order to have performance indices for comparison between other same-dof parallel manipulator.

References

[1] Merlet, J. –P. (2006) Parallel Robots, Springer.

[2] Masory, O. and Wang, J. (1995) Workspace evaluation of Stewart platforms, *Advanced Robotics Journal* **9**, 443- 461.

[3] Yoshikawa, T. (1985) Manipulability of robotic mechanisms, Int. J. Robot. Res., **4**, 3–9.

[4] Salisbury, J. K., and Craig, J. J. (1982) Articulated hands: Force control and kinematic issues, Int. J. Robot. Res., **4**, 4–17.

[5] Ranjbaran, F., Angeles, J., Gonzalez-Palacios, M. A. and Patel, R. V. (1995) The mechanical design of a seven-axes manipulator with kinematic isotropy, *Journal of Intelligent and Robotic Systems.*, **14**, 21-41.

[6] Gosselin, C.M. (1992) The optimum design of robotic manipulators using dexterity indices, *Journal of Robotics and Autonomous Systems*, **9**, 213–226.

[7] Kim, S. G. and Ryu, J. (2003) New dimensionally homogeneous jacobian matrix formulation by three end-effector points for optimal design of parallel manipulators, IEEE Transactions on Robotics and Automation, **19**, 731–737.

[8] Pond, G. and Carretero, J.A. (2007) Quantitative dexterous workspace comparison of parallel manipulators, Mechanism and Machine Theory, **42**, 1388-1400.

[9] Angeles, J. (2006) Is there a characteristic length of a rigid-body displacement?, Mechanism and Machine Theory, **41**, 884–896.

[10] Hosseini, M.A. and Daniali, H.M. (2011) Weighted local conditioning index of a positioning and orienting parallel manipulator, Sientica Iranica B, **8**, 115-120.

[11] Hosseini, M.A., Daniali, H.R. M. and Taghirad, H.D. (2011) Dexterous Workspace optimization of Triceps Parallel Manipulator, Advanced Robotics, **25**, 1697-1712.

[12] Zlatanov, D., Bonev, I.A. and Gosselin, C.M. (2002) Constraint Singularities of Parallel Mechanisms, IEEE International Conference on Robotics and Automation (ICRA 2002), Washington, D.C., USA, May, 11–15.

[13] Hosseini, M.A. and Daniali, H.M. (2011) Machine Tool Design Optimization of High Resolution Parallel Hexapod in Cartesian Workspace, *Majlesi Journal of Mechanical Engineering*, **4**, 75-84.